Systems/Circuits

Hippocampal Inputs in the Prelimbic Cortex Curb Fear after Extinction

Weronika Szadzinska, Konrad Danielewski, Kacper Kondrakiewicz, Karolina Andraka, Evgeni Nikolaev, Marta Mikosz, and Ewelina Knapska

Laboratory of Emotions Neurobiology, Nencki-European Molecular Biology Laboratory Partnership for Neural Plasticity and Brain Disorders BRAINCITY, Nencki Institute of Experimental Biology, Pasteur 3 Str., 02-093 Warsaw, Poland

In contrast to easily formed fear memories, fear extinction requires prolonged training. The prelimbic cortex (PL), which integrates signals from brain structures involved in fear conditioning and extinction such as the ventral hippocampus (vHIP) and the basolateral amygdala (BL), is necessary for fear memory retrieval. Little is known, however, about how the vHIP and BL inputs to the PL regulate the display of fear after fear extinction. Using functional anatomy tracing in male rats, we found two distinct subpopulations of neurons in the PL activated by either the successful extinction or the relapse of fear. During the retrieval of fear extinction memory, the dominant input to active neurons in the PL was from the vHIP, whereas the retrieval of fear memory, regardless of the age of a memory and testing context, was associated with greater BL input. Optogenetic stimulation of the vHIP–PL pathway after one session of fear extinction increased conditioned fear, whereas stimulation of the vHIP inputs after several sessions of extinction decreased the conditioned fear response. This latter effect was, however, transient, as stimulation of this pathway 28 d after extinction increased conditioned fear response again. The results show that repeated fear extinction training gradually changes vHIP–PL connectivity, making fear suppression possible, whereas in the absence of fear suppression from the vHIP, signals from the BL can play a dominant role, resulting in high levels of fear.

Key words: **basolateral amygdala; fear extinction; fear memory; prefrontal cortex; prelimbic cortex; ventral hippocampus**

Significance Statement

Behavioral therapies of fear are based on extinction learning. As extinction memories fade over time, such therapies produce only a temporary suppression of fear, which constitutes a clinical and societal challenge. In our study, we provide a framework for understating the underlying mechanism by which extinction of fear memories fade by demonstrating the existence of two subpopulations of neurons in the prelimbic cortex associated with low and high levels of fear. Insufficient extinction and exposure to the context in which fear memory was formed promoted high fear neuronal activity in the prelimbic cortex, leading to fear retrieval. Extensive extinction training, on the other hand, boosted low fear neuronal activity and, as a result, extinction memory retrieval. This effect was, however, transient and disappeared with time.

Introduction

Having flexibility to adjust emotional responses to a changing environment is a critical component of normal behavior. In the absence of an imminent threat, when fear is no longer adaptive, its expression can be suppressed by extinction, that is, the repeated presentation of a stimulus associated with fear, conditioned stimulus (CS), in the absence of an aversive event (Maren, 2011). It is thought that extinction is a form of new learning and therefore leads to competition between fear and extinction memories (Konorski, 1948; Bouton, 1993; Rescorla, 2004; Bouton, 2004). In contrast to fear memory, which can be formed instantly (Ohman et al.,1975) and is easily retrieved throughout the entire lifetime of an animal (Gale et al., 2004), formation of fear extinction memory requires a significant number of trials, and its retrieval becomes more difficult with the passage of time (Bouton, 2002; Bouton et al., 2006).

Human and animal studies implicated the medial prefrontal cortex (mPFC) in regulation of fear based on previously learned information. In particular, the dorsal part, the prelimbic cortex (PL), has been associated with retrieval of fear memory

Received Apr. 2, 2020; revised July 23, 2021; accepted July 29, 2021.

Author contributions: E.K. designed research; W.S., K.D., K.K., K.A., and M.M. performed research; W.S., K.D., K.K., K.A., E.N., M.M., and E.K. analyzed data; and E.K. wrote the paper.

This work was supported by grants from the National Science Center (2011/01/D/NZ3/02149 and 2013/08/W/NZ4/00691) and the Foundation for Polish Science (MAB/2018/10): The Nencki-European Molecular Biology Laboratory Center of Excellence for Neural Plasticity and Brain Disorders BRAINCITY project, carried out within the International Research Agendas program of the Foundation for Polish Science, supported by the European Union under the European Regional Development Fund.

The authors declare no competing financial interests.

Correspondence should be addressed to Ewelina Knapska at e.knapska@nencki.edu.pl.

https://doi.org/10.1523/JNEUROSCI.0764-20.2021

(Burgos-Robles et al., 2009; Sierra-Mercado et al., 2011; Giustino and Maren, 2015). The PL receives inputs from the basolateral amygdala (BL), a brain region storing memories of both fear and fear extinction (Fanselow and LeDoux, 1999) and the ventral hippocampus (vHIP), a structure critical for the contextual gating of fear responses (Barad et al., 2006; Hoover and Vertes, 2007; Ji and Maren, 2007). It has been shown that after fear extinction, the BL promotes fear signaling in the PL (Sotres-Bayon et al., 2012; Senn et al., 2014). Similarly, activation of the vHIP–PL pathway has been associated with retrieval of fear memory (Orsini et al., 2011; Jin and Maren, 2015; Wang et al., 2016; Kim and Cho, 2017) and increased anxiety (Adhikari et al., 2010; Padilla-Coreano et al., 2016; Parfitt et al., 2017). On the other hand, some reports have also indicated that the vHIP–PL pathway can reduce fear (Sotres-Bayon et al., 2012; Vasquez et al., 2019); however, the exact role of this pathway in expression and extinction of conditioned fear is not known. Little is also known about how the PL integrates information from the BL and vHIP after extinction occurred.

Here, we study the role of the BL and vHIPP signals in the PL in rats tested for recent and remote fear extinction memory using immunohistochemistry, functional connectivity tracing, and optogenetics. CS presentation outside the extinction context results in the recovery of the previously conditioned fear response (fear renewal) (Bouton et al., 2006). Because extinguished fear is context dependent, we systematically compared patterns of activation and connectivity in both the extinction and conditioning contexts. Regardless of the age of a fear extinction memory and the testing context, in animals with high levels of fear, the activated neurons within the PL were innervated mainly by the BL. In contrast, low levels of fear were associated with activation of neurons that receive dominant projections from the vHIP. Because the vHIP input to the PL has been previously shown to both increase freezing and reduce fear (Kim and Cho, 2017), we tested the effects of optogenetic stimulation of the vHIP–PL pathway. We observed that after one session of fear extinction, vHIP–PL activation leads to an increased display of fear. However, after several sessions of extinction, the effect is the opposite. These results show that extensive fear extinction training gradually rebuilds vHIP–PL connectivity, making fear suppression possible. This effect is, however, transient and disappears with time.

Materials and Methods

Animals

In all experiments, male Long-Evans, Wistars, or PSD-95:Venus transgenic rats (220–400 g at the beginning of the experiment) bred in the Nencki Institute Animal House were used. Animals were housed individually in transparent plastic cages placed on standard stainless steel racks. Rats had access to water and food *ad libitum* and were kept under a 12/12 light/dark cycle. Behavioral experiments were performed during the light phase. All procedures were followed in accordance with the Polish Act on Animal Welfare, after obtaining specific permission from the First Warsaw Ethical Committee on Animal Research.

PSD-95:Venus transgenic rats

PSD-95:Venus transgenic rats were used for visualization of synapses in activated neurons. The construct allows the dendrites and synapses of activated neurons to be visualized with fluorescent tags by encoding PSD-95 (a major component of postsynaptic densities), an *Arc* UTR, dendrite localizing sequences, a c-Fos promoter (which makes the expression dependent on neuronal activation), and Venus reporter protein. The reporter protein is placed under the control of a shortened c-Fos sequence (encoding only the first four amino acids of c-Fos) and therefore lacks the nuclear localization signal. Such an approach preserves promoter inducibility, allowing for the visualization of neuronal morphology (Knapska et al., 2012).

Surgical procedures

Functional anatomy tracing. Six or 7 d before behavioral training, rats received bilateral intracranial injections of the anterograde axonal transport tracers tetrame-thylrhodamine, FluoroRuby (FR), and PHA-L Alexa Fluor 647 conjugate (Invitrogen) into the BL and vHIP. The sides of the injection and the type of the tracer were counterbalanced between the brain structures. All surgical instruments were sterilized before surgery. Rats were anesthetized with isoflurane (Aerane). Ocular lubricant was used to moisten the eyes, and the scalp was shaved. After being placed into the stereotaxic apparatus (David Kopf Instruments), the scalp was disinfected with 70% (v/v) alcohol, incised, and retracted. Two small burr holes were drilled to allow a Hamilton syringe needle (1 μL) to be lowered into the desired part of the brain. The coordinates used were as follows: BL [anteroposterior (AP), −2.2; mediolateral (ML), ±4.8; dorsoventral (DV), −8.6], vHIP (AP, −5.3; ML, ±5.5; DV, −7.0), FR [10% (w/v) solution in distilled water], and PHA-L [2.5% (w/v) solution in 0.1 M sodium PBS, pH 7.4] were delivered into the BL and vHIP with the use of a Hamilton syringe (Microsyringe Pump, World Precision Instruments), 0.5 μL total volume, 25 nL/min for 20 min; the needle remained in place for another 20 min to allow for the diffusion of the tracer. After the injection, the incision was sutured and treated with an antibiotic ointment, and the animals were administered an analgesic (Tolfedine, 4 mg/kg s.c.). To avoid dehydration, the animals were given 1 ml of warm 0.95% NaCl/100 × g of body weight by subcutaneous injection. The rats were kept on a heating pad until they recovered from anesthesia before returning to their home cages. The animals were allowed 6–7 d of postoperative recovery.

Virus injections and optic fibers implantations. The adeno-associated virus (AAV) vector used, rAAV5 CaMKIIα-hChR2 (H134R)-EYFP, was purchased from Addgene. Viral titers were 5.24 × 1011 particles/ml. Fourteen days before the behavioral training, the experimental and control rats received bilateral intracranial injections of the virus (experimental: rAAV5 CaMKIIα-hChR2 (H134R)-EYFP; control: rAAV5 CaMKIIα (H134R)-EYFP) into the vHIP. Rats were anesthetized with isoflurane (Aerane), and an analgesic was administered (Butomidor, 1 mg/kg s.c.). Ocular lubricant was used to moisten the eyes, the scalp was shaved, and 2% lidocaine gel was applied. After being placed into the stereotaxic apparatus (Stoelting), the scalp was disinfected with 70% (v/v) alcohol, incised, and retracted. Two small burr holes were drilled to allow for a NanoFil 35GA beveled needle (model #NF35BV-2, World Precision Instruments) to be lowered into the desired part of the brain, and another two holes were drilled over the PL to allow optic fiber application. The coordinates used were as follows: PL, AP +3.2, ML ±0.6, DV −2.2; vHIP, AP −5.3, ML ±5.5, DV −7.0. An additional three small holes were drilled, and three skull screws were placed to secure a cement cap. The virus was delivered using a NanoFil syringe and infusion pump (Microsyringe Pump, World Precision Instruments) volume 250 nl, speed 100 nl/min for 5 min; the needle remained in place for another 5 min to allow for the virus diffusion. After injection, the optic fiber cannulas were mounted (model #UM22-100, Thorlabs) 0.22 numerical aperture (NA), 100 μm core, placed in Ceramic Ferrules (model #CFLC128-10, Thorlabs), connected to self-made threaded covers with Data Optics Hysol epoxy glue 0151. Optic fibers were inserted bilaterally into the PL at an angle of 20° to prevent stimulation of the infralimbic cortex. Then the exposed skull was coated with dental cement. All the animals were administered an analgesic/anti-inflammatory (Tolfedine, 4 mg/kg, s.c.) and antibiotic (Baytril, 2.5 mg/kg, s.c.). To avoid dehydration, the animals were given 1 ml of warm 0.9% NaCl/100 × g of body weight by subcutaneous injection. The rats were kept on a heating pad until they recovered from anesthesia before returning to their home cages.

Behavioral apparatus

Modular conditioning chambers (VFC-008 Standard Fear Conditioning Chamber or ENV-008 Standard Modular Test Chamber, Med Associates) were used for all phases of the experiment. The floor of the chamber was equipped with stainless steel rods wired to a shock source and a solid-state grid scrambler (Med Associates) for footshock [unconditioned stimulus

(US)] delivery. Stainless steel pans were placed underneath the grid floor before the animals were placed inside the box. The chambers were lit with house lights. A speaker mounted in one of the chamber walls was used for the delivery of the acoustic conditioned stimuli (CSs). Sensory stimuli were adjusted within these chambers to generate two distinct contexts, A and B. For context A, a house light mounted in the ceiling of the cage was illuminated, and the room lights remained on. The chambers were cleaned with a 1% ammonium hydroxide solution, and stainless steel pans containing a thin film of the same solution were placed underneath the grid floors. This was done before the rats were placed inside to provide a distinct odor. Ventilation fans supplied background noise (65 dB). For context B, all room and chamber house lights were turned off as were the ventilation fans, and the computer screen provided illumination. White Plexiglas floors were placed on the grid of each chamber, and chambers were cleaned with a 1% acetic acid solution. Stainless steel pans containing a thin film of this solution were placed underneath the floors before the rats were placed inside. In the ENV-008 Standard Modular Test Chamber, animal behavior was recorded with an IP camera (AXP CUBE P2P S, Alexim) equipped with a fish-eye objective and placed in front of the transparent front door of the chamber. Video was then digitized by a computer system. Freezing was defined as the cessation of all movement, except what was required for respiration, for at least 1 s. The freezing recognition software converted the cumulative time spent freezing into a percentage score. For the experiments performed in VFC-008 Standard Fear Conditioning Chambers, freezing was analyzed with the software delivered by Med Associates (c-Fos mapping and functional anatomy tracing experiments), whereas freezing recorded in the ENV-008 Standard modular test chamber (optogenetic experiments) was analyzed with Beha Active software (http://www.pmbogusz.net/).

Behavioral training and testing

c-Fos *Mapping.* Rats were submitted to three phases of training: fear conditioning, extinction, and retrieval testing. For fear conditioning, rats were placed in the conditioning chambers in context A. The rats received five tone (10 s, 80 dB, 2 kHz) footshock (1 s, 1 mA) trials [70 s intertrial interval (ITI)] beginning 3 min after being placed in the chambers. Sixty seconds after the final shock, the rats were returned to their home cages. Twenty-four hours after the conditioning session, rats were subjected to fear extinction, which consisted of the conditioned tone in a novel context (B). Rats received 45 CS presentations (10 s, 80 dB, 2 kHz, 70 s ITI) 2 min after placement in the context. Testing took place 1 or 28 d after the extinction training in context A or B.

Functional anatomy tracing. Rats were subjected to fear conditioning and extinction sessions as described above. Testing took place 5 or 28 d after the extinction session, either in context A or B. Five days is the time period required for the expression of the PSD-95:Venus fusion protein to go back to the basal level following induction by fear conditioning and extinction (compare Knapska et al., 2012).

Optogenetic experiments. In the first set of experiments (see Fig. 3), rats were subjected to the fear conditioning and extinction sessions as described above. The first group was submitted to fear conditioning and one extinction session, and the second group to fear conditioning and two extinction sessions. Testing consisted of 21 CS presentations that started 2 min after the placement of rats in the chambers, 1 d after the last extinction session. In the three consecutive blocks, the first two CSs (10 s, 80 dB, 2 kHz, 60 s ITI) were not paired with any stimulation, whereas the following five CSs were paired with optogenetic stimulation (473 nm, 10 mW, 5 ms pulses, 20 Hz). The light stimulation began 10 s before the CS presentation. In addition, a control group was included in each of the experiments—rats injected with the control virus not containing channelorhodopsin. Fear level was assessed during the extinction and testing sessions by measuring time spent freezing during the CS presentation.

In the second set of experiments (see Fig. 4), rats were subjected to the fear conditioning and extinction sessions as described above. The first group was subjected to a fear conditioning session and tested without fear extinction on two subsequent days (context B and context A, respectively). On the next day, the animals were subjected to the extinction session. The second group was subjected to fear conditioning, two sessions of fear extinction on 2 consecutive days, testing on 2 subsequent days (context B and context A, respectively), and the third session of extinction with stimulation. Then the rats were tested again after 28 d in context B and context A on 2 subsequent days. Testing consisted of 10 CSs (10 s, 80 dB, 2 kHz, 60 s ITI) presentations, the first five without laser stimulation and the following five with laser stimulation synchronized with the CS onset (473 nm, 10 mW, 5 ms pulses, 20 Hz). The extinction session with stimulation consisted of 45 CS presentations in an alternating pattern of five CS blocks without and with stimulation. The control group, rats injected with the control virus not containing channelorhodopsin, was included in each of the experiments. Fear level was assessed during the extinction and testing sessions by measuring time spent freezing during the CS presentation. When the level of freezing was very low, time spent in relaxed posture was measured. Relaxed posture has been previously described as "animal resting on their legs in a ball-shaped posture with the animals resting on their legs with the tail around the body and the head mostly in a vertical position (Tang et al., 2001). The video recordings were analyzed by the observer blind to the experimental condition, who assessed freezing and relaxed posture when the CSs were presented.

Optogenetic stimulation. A laser with a wavelength of 473 nm and maximum output of 100 mW (Omicron Laserage) was used. The light was delivered through a rotary joint (Doric Lenses) to two optic fibers (core 200 μm, NA 0.37, 2 m in length; Thorlabs) and from there to thread-attached self-made optic fiber cannulas. The typical laser power at the cannula tip was 10 mW. The laser onset was triggered by transistor-transistor logic (TTL) output from the conditioning chamber (Med Associates). The laser pulsation (5 ms pulse duration, 20 Hz) was controlled by an Arduino board. The laser power output was measured using a commercial power meter (model #PM200 with S121C sensor, Thorlabs).

c-Fos *Immunohistochemistry.* Rats were anesthetized with an overdose of sodium pentobarbital and perfused intracardially with ice-cold PBS, pH 7.4, followed by 4% paraformaldehyde in 0.1 M phosphate buffer, pH 7.4. The brains were removed and stored in the same fixative for 24 h at 4°C and subsequently immersed in 30% sucrose at 4°C. The brains were then slowly and gradually frozen and sectioned at 40 μm on a cryostat. The coronal brain sections containing the BL, vHIP, and PL were collected. The immunohistochemical staining was performed on free-floating sections. The sections were washed three times in PBS, pH 7.4, incubated for 10 min in 0.03% H_2O_2 in PBS, washed twice in PBS, and incubated with a polyclonal antibody (anti-c-Fos, sc-52, 1:1000; Santa Cruz Biotechnology), in PBS and normal goat serum (3%; Vector) for 48 h at 4°C. The sections were then washed three times in PBS with 0.3% Triton X-100 (Sigma), incubated with goat anti-rabbit biotinylated secondary antibody (1:500; Vector) in PBS/Triton and normal goat serum (3%) for 2 h at room temperature, washed three times in PBS/Triton, incubated with avidin-biotin complex (1:1000 in PBS/Triton; ABC Kit, Vector Labs) for 1 h at room temperature, and washed three times in PBS. The immunostaining reaction was developed using the oxidase-diaminobenzidine-nickel method. The sections were incubated in distilled water with diaminobenzidine (DAB; Sigma), 0.5 M nickel chloride, and peroxidase (Sigma) for 5 min. The staining reaction was stopped by three washes with PBS. The reaction resulted in a dark-brown stain within the nuclei of c-Fos immunoreactive neurons. The sections were mounted on slides, air dried, dehydrated in ethanol solutions and xylene, and coverslipped with Permount (Fisher Chemical).

c-Fos+*GAD67 Immunohistochemistry.* The immunohistochemical staining was performed on free-floating sections. The sections were washed three times in PBS, pH 7.4, incubated for 10 min in 0.03% H_2O_2 in PBS, washed once in PBS, incubated for 1 h in 10% NGS with PBS and incubated with a polyclonal antibody (anti-c-Fos, sc-52, 1:1000; Santa Cruz Biotechnology) and anti-GAD67 (1:4000; Merck Millipore, catalog #MAB5460) in PBS for 96 h at 4°C. Sections were then washed three times in PBS with 0.3% Triton X-100 (Sigma), incubated with goat anti-rabbit biotinylated secondary antibody (1:1000; Vector Labs) in PBS for 2 h at room temperature, washed three times in PBS/Triton, incubated with avidin-biotin complex (1:1000 in PBS; ABC Kit, Vector Labs) for 1 h at room temperature, and washed three times in PBS. The immunostaining

reaction was developed using the oxidase-diaminobenzidine-nickel method. The sections were incubated in distilled water with DAB (Sigma), 0.5 M nickel chloride, and peroxidase (Sigma) for 5 min. The staining reaction was stopped by three washes with PBS. The sections were incubated in PBS overnight. The following day, sections were incubated for 2 h with secondary goat anti-mouse antibody (1:1000; Vector Labs) in PBS, washed three times in PBS/Triton, incubated with avidin-biotin complex (1:500 in PBS; ABC Kit, Vector Labs) for 1 h at room temperature, and afterward washed three times with PBS. Subsequent sections were stained using VIP purple kit (catalog #SK-4600, Vector Labs). The reaction was stopped after 1–2 min by three washes in PBS. The reaction resulted in a black stain within the nuclei of c-Fos immunoreactive neurons and a purple stain in cell bodies of GAD67-positive cells. The sections were mounted on slides, air-dried, dehydrated in xylene, and coverslipped with Entellan (Merck Millipore).

Fluorescent immunostaining for GFP. The immunofluorescent staining was performed on free-floating sections. The sections were washed with PBS with 0.2% Triton X-100 (PBST), blocked with 5% (v/v) normal donkey serum in PBST, and incubated overnight at 4°C with anti-GFP rabbit antibody (Invitrogen) diluted with 1% normal donkey serum in PBST. The next day, sections were rinsed with PBST before 1 h incubation at room temperature with a secondary antibody conjugated to Alexa Fluor 488 (1:500; Invitrogen). After several washes, the sections were mounted onto glass slides, air-dried, overlaid with Vectashield Mounting Medium, and covered with a glass coverslip.

Image capture and analysis

The measure of c-Fos immunopositivity was expressed as density, determined in the following manner. For each brain section, the number of c-*fos* immunopositive nuclei in areas of interest was counted and divided by the area occupied by the structure (in millimeters squared). Image analysis was done with the aid of a Nikon Eclipse Ni-U microscope and an image analysis computer program (ImageJ) on two sections per animal brain. Boundaries of each structure were defined with the use of the Paxinos atlas (Paxinos and Watson, 2007). The dorsal and ventral borders of the PL were defined by the shape of the corpus callosum, which served as a guideline for choosing the appropriate corresponding atlas plate. For the BL, the shape of the amygdala itself was used as a guideline, whereas for the vHIP, the shape of the hippocampus indicated the exact boundaries of the structure.

The triple-labeling results were analyzed with the aid of confocal laser-scanning microscopy. The confocal system consisted of an Inverted Leica SP5 DMI6000 microscope, equipped with an Ar laser producing light at 488 nm, a HeNe laser for 568 nm, and a HeNe laser for 647 nm of light. Two objectives (40×) were used to scan the samples. A series of continuous optical sections at 1 μm intervals along the *z*-axis of the tissue section were scanned for all three fluorescent signals. The signal obtained for each fluorophore on one series of optical sections was stored separately as a series of 1024 × 1024 pixel images. The images were then processed with Imaris 6.3.1 software (Bitplane). PHA-L- and FR-labeled images were separately combined with Venus-stained cell bodies and proximal dendrites to analyze for the presence of close appositions between PHA-L- or FR-stained terminals and Venus-positive neurons in the PL. For the location of the PL for the confocal imaging, the shape of the corpus callosum was used as an indicator of the plate from the Paxinos atlas (Paxinos and Watson, 2007). This was used to calculate the distance, measured in micrometers, from the highest point of the slice above the PL to its actual dorsal boundary.

Afferent terminals on Venus-positive neurons were analyzed in two scan images taken bilaterally for the vHIP/BL-injected rats under a 40× objective within the PL (2.20–3.70 mm from bregma). The potential contacts between PHA-L- and FR-labeled fibers and the Venus-positive neurons were estimated as numbers of voxels for axonal varicosities located in close proximity to Venus-positive neurons. Then the ratios of vHIP/BL projections (measured in voxels) were calculated for single Venus-positive neurons within the PL and represented as the percentage of neurons with a certain BL/vHIP input ratio onto the active cells in the PL. The overall projections from the vHIP and BL to the PL were analyzed for the same images as projections to the activated neurons. The ratio of vHIP/BL (measured in voxels) was then calculated.

Histology

Animals were deeply anesthetized with an overdose of sodium pentobarbital (100 mg/kg) and perfused intracardially with 0.01 M PBS (200 ml) and 4% PFA (in PBS, 300 ml). Brains were stored for 24 h in PFA, then for 3 d in 30% sucrose and sectioned with a freezing microtome into 40 μm slices. EYFP (enhanced yellow fluorescent protein) expression in injection sites and fiber optic placement was checked for each animal.

Electrophysiological recordings. The electrophysiological signal was recorded with a Neuropixels 1.0 probe inserted into the mPFC of an urethane-anaesthetized rat. Simultaneously the vHIP was stimulated with a bipolar electrode (stainless steel, 2 × 126 μm) every 10 s (single pulse, 0.1 ms, 0.1 mA). After spike sorting (using Kilosort2 and Phy2), responses of each neuron to the stimulation were tested using ZETA method (Montijn et al., 2020). The MATLAB functions provided by the authors of the method (https://github.com/JorritMontijn/ZETA) allowed to test (1) which neurons responded in a 2–100 msec time window to the stimulation, with either an increase or decrease in the firing rate, $p < 0.001$ and (2) what the average latency (Zeta) of the response was for each neuron.

Statistical analyses. Statistical analyses of raw data were performed with GraphPad Prism 6 or Statistica 7.0 software. The time animals spent freezing during the CS was transformed into percentage values. The datasets that did not meet the criteria for parametric analyses (tested with the Shapiro–Wilk normality test) were subjected to nonparametric testing with the Mann–Whitney test or Kruskal–Wallis test followed by Dunn's multiple comparisons test. The parametric analyses were performed with repeated-measures ANOVAs followed by Fisher's least significant difference (LSD) or Newman–Keuls tests for multiple comparisons. For the optogenetic stimulation experiments, two factors were compared using a mixed two-way ANOVA with repeated measures, the experimental versus control group and light stimulation versus no-light stimulation. The Kolmogorov–Smirnov two-sample test was performed to compare differences between the rate of afferent projections from the BL and vHIP onto activated neurons in the PL for all experimental groups. Cumulative frequency distributions for each group were made with the same 10 intervals (0–0.2, 0.2–0.4, 0.4–0.6, 0.6–0.8, 0.8–1.0, and 1.2–1.4, 1.4–1.6, 1.6–1.8, 1.8–2.0, and > 2.0) used for each distribution. The number of cells used for the cumulative frequency distributions comparison were the following: Extinction group, 149; Fear Renewal 1 group, 122; Spontaneous Recovery group, 148; Fear Renewal 28 group, 113. The test focused on the largest of the observed deviations. The following numbers of outliers were removed: four outliers with freezing levels indicating a different emotional state from the rest of the experimental group. The criterion for statistical significance was a probability level of $p < 0.05$.

Results

We mapped neuronal activation in the vHIP and BL in rats tested for a recent and remote fear extinction memory 1 d and 28 d after the extinction session, respectively, tested in an extinction (B) or conditioning (A) context: Extinction 1 d, Fear Renewal 1 d, Spontaneous Recovery, Fear Renewal 28 d groups. For the control groups we used animals that were not subjected to fear conditioning, but except for footshocks, were exposed to the same contexts and stimuli as the experimental groups (No Conditioning 1 and No Conditioning 28; Fig. 1). We found that retrieval of the recent extinction memory in the extinction context led to a low level of fear and increased activation of the vHIP (Figure 1*B*,*C*; analysis of the level of freezing, Kruskal–Wallis test, $H = 33.13$, $p < 0.0001$, followed by Dunn's test; Extinction 1 vs Fear renewal 1, $p < 0.05$; No Conditioning 1 vs Fear renewal 1, $p < 0.001$; analysis of c-Fos expression in vHIP, one-way ANOVA, $F_{(5,40)} = 4.44$, $p = 0.0026$, followed by Fisher's LSD test;

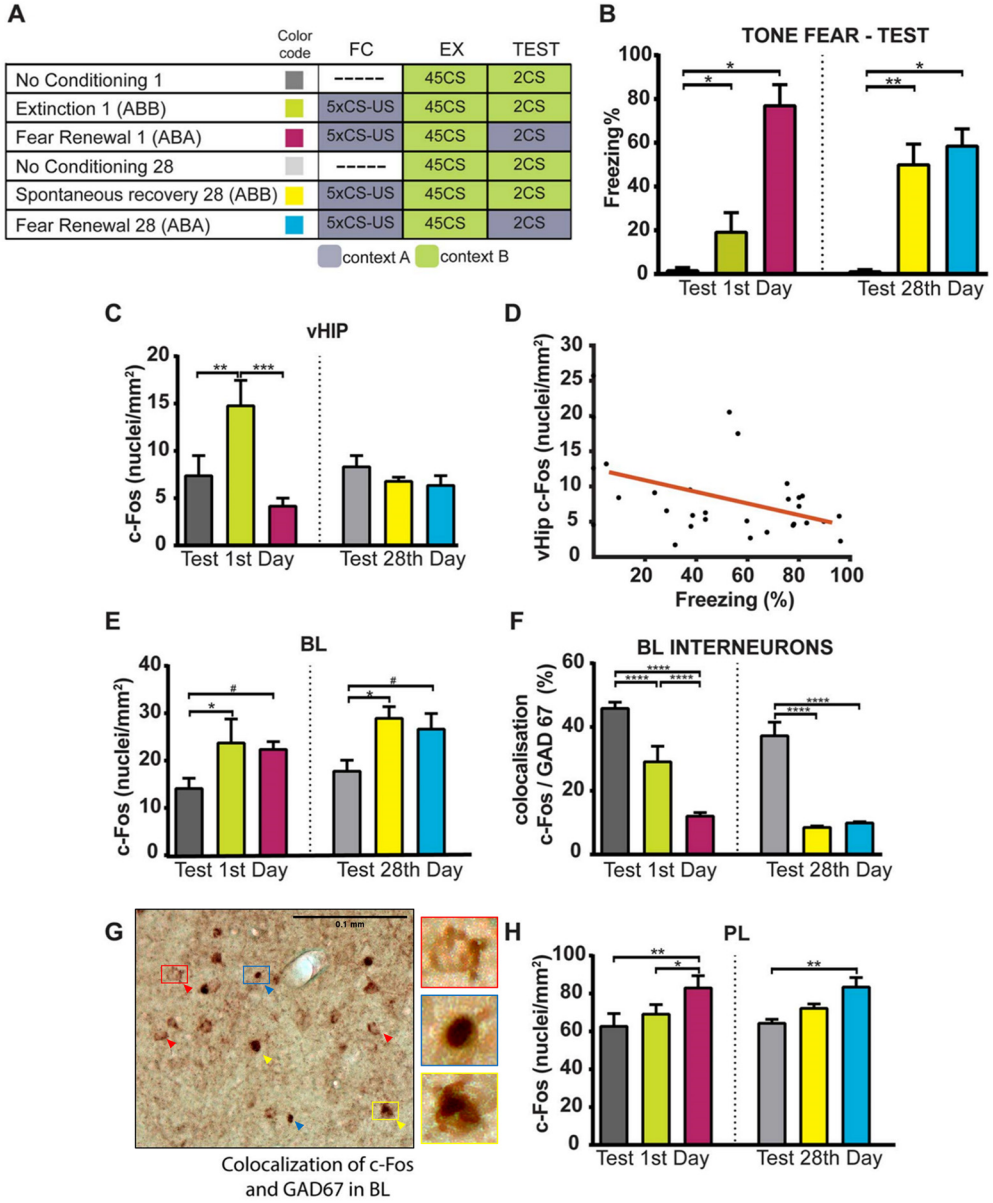

Figure 1. Successful retrieval of fear extinction memory, in contrast to retrieval of fear memory, is associated with increased activation of the vHIP. ***A***, Scheme of the behavioral training. ***B***, The level of fear during the memory retrieval sessions on test day (measured as percentage of freezing during the CSs, $n = 8–10$). ***C***, Activation of the vHIP ($n = 8–9$). ***D***, Negative correlation between levels of freezing and c-Fos expression in the vHIP. ***E***, Activation of the BL ($n = 7–8$). ***F***, Activation of the inhibitory neurons in the BL ($n = 8–10$). ***G***, An example of the cells labeled for c-Fos and GAD67; red arrows, GAD67-positive/c-Fos-negative cells; blue arrows, c-Fos-positive/GAD67-negative cells; yellow arrows, c-Fos-positive and GAD67-positive cells. Right, Magnified examples of respective cells. ***H***, Activation of the PL ($n = 7–8$). Error bars indicate mean ± SEM; $^{\#}p = 0.05$, $*p < 0.05$, $**p < 0.01$, $***p < 0.001$, $****p < 0.0001$. 1, 28, Rats tested for recent and remote fear extinction memory 1 or 28 d after the extinction session; FC, fear conditioning; EX, fear extinction; US, unconditioned stimulus.

Extinction 1 vs Fear renewal 1, $p = 0.002$; Extinction 1 vs No Conditioning 1, $p = 0.0026$).

Exposure to the same experimental conditions 4 weeks after extinction resulted in spontaneous recovery of fear, which manifested as a significant increase in the freezing level and no increase in vHIP activation (analysis of the level of freezing, Kruskal–Wallis test, $H = 33.13$, $p < 0.0001$, followed by Dunn's test; Spontaneous recovery 28 vs No Conditioning 28, $p < 0.01$). The number of activated neurons in the vHIP was negatively correlated with the level of fear (Figure 1*D*; Pearson's correlation coefficient $r = -0.45$, $p < 0.05$). In contrast, the BL was activated in animals with both low and high fear levels (Fig. 1*E*; one-way ANOVA, $F_{(5,41)} = 3.32$, $p = 0.0131$, followed by Fisher's LSD test; Extinction 1 vs No Conditioning 1, $p = 0.0288$; Spontaneous Recovery 28 vs No Conditioning 28, $p = 0.0122$). There was also a trend toward an increase in Fear renewal 1 versus No Conditioning 1, $p = 0.059$, and Fear renewal 28 versus No Conditioning 28, $p = 0.0508$ comparisons. However, as the activation mapping method we used (c-Fos expression) labels both excitatory projection neurons and inhibitory interneurons, it is not clear which type of the BL neurons was involved. To investigate what type of neurons was activated by retrieval of fear and extinction memories, we analyzed colocalization of c-Fos and GAD67, a marker of inhibitory neurons, in activated cells (Fig. 1*F*,*G*). This analysis showed that fewer inhibitory neurons in the BL were activated in fear-provoking conditions (in Fear Renewal 1, Spontaneous Recovery, and Fear Renewal 28 groups) than in the low fear

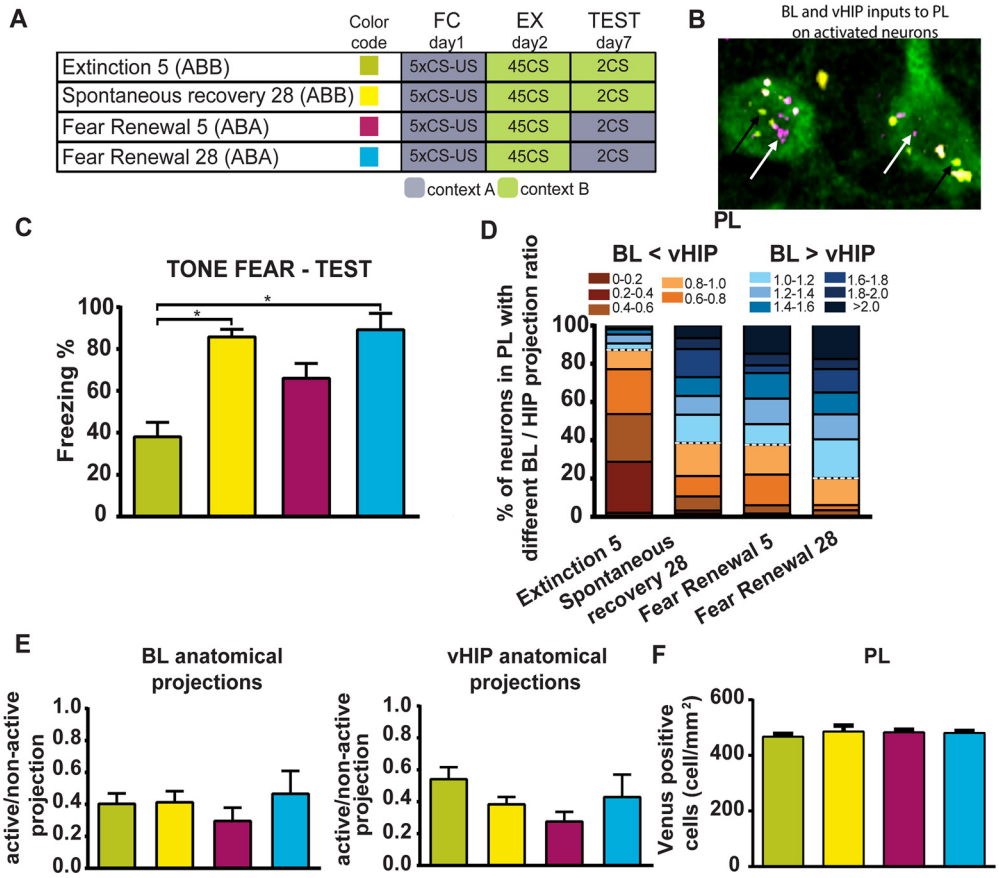

Figure 2. High level of fear is associated with activation of the PL neurons innervated by the BL; low level of fear is associated with activation of the PL neurons receiving vHIP inputs. ***A***, Scheme of the behavioral training. ***B***, Example of the active neurons expressing PSD-95:Venus fusion protein under control of the *c-fos* promoter and receiving inputs from the BL and vHIP (green, PSD-95:Venus fusion protein; magenta, vHIP projections marked with PHA-L (white arrow); yellow, BL projections marked with FluoRuby (black arrow). ***C***, The level of fear during the memory retrieval sessions (measured as percentage of freezing during the CSs, $n = 4–5$). ***D***, Percentage of activated neurons with different ratios of BL/vHIP projections plotted for each experimental group. ***E***, Ratio of the active projections (cells where tracers from the BL/vHIP overlap with c-*fos* expression) over the anatomic projections from the BL or vHIP (overall number of cells in PL that show tracers labeling). ***F***, Quantification of Venus-positive cells in all behavioral groups. Error bars indicate mean ± SEM; $*p < 0.05$. 5, 28, Rats tested for recent or remote fear extinction memory 5 or 28 d after the extinction session; FC, fear conditioning; EX, fear extinction.

conditions (No Conditioning 1, No Conditioning 28, and Extinction 1 groups; one-way ANOVA, $F_{(5,44)} = 34.66$, $p < 0.0001$, followed by Fisher's LSD test; No Conditioning 1 vs Extinction 1, $p < 0.0001$; Extinction 1 vs Fear Renewal 1, $p < 0.0001$; No Conditioning 1 vs Fear Renewal 1, $p < 0.0001$; No Conditioning 28 vs Spontaneous recovery 28, $p < 0.0001$; No Conditioning 28 vs Fear Renewal 28, $p < 0.0001$). As the number of activated (c-Fos positive) cells in the BL in the Extinction 1, Fear Renewal 1, Spontaneous Recovery, and Fear Renewal 28 groups was similar, this suggests that a high level of fear recruits more BL projection neurons. Next, we compared neuronal activation of the PL in all tested groups (Fig. 1*H*). Consistent with our previous results (Knapska and Maren, 2009), increased activation of the PL was observed only in rats exposed to the conditioning context, regardless of the age of the fear extinction memory (one-way ANOVA, $F_{(5,41)} = 3.35$, $p = 0.0125$, followed by Fisher's LSD test; Fear renewal 1 vs No Conditioning 1, $p < 0.01$; Fear renewal 28 vs No Conditioning 28, $p < 0.01$).

To further characterize neurons in the PL activated by the retrieval of extinction memory, spontaneous recovery of fear, and fear renewal, we traced the functional projections from the vHIP and BL to the PL (Fig. 2*A–D*). We used transgenic rats expressing a PSD-95:Venus fusion protein under the control of a *c-fos* promoter injected with anterograde tracers into the vHIP and the BL (compare Knapska et al., 2012). We found two distinct subpopulations of neurons within the PL that were activated by low and high levels of fear, which can be distinguished by their projections from the vHIP and BL. For the cells in the PL whose activity was correlated with low freezing, inputs were coming mainly from the vHIP. For neurons whose activity was correlated with elevated freezing, during both spontaneous recovery of fear and fear renewal, we observed preferential innervation by the BL (analysis of the level of freezing, Kruskal–Wallis test, $H = 11.6$, $p = 0.001$ followed by Dunn's test; Extinction 5 vs Spontaneous recovery 28, $p < 0.05$; Extinction 5 vs Fear renewal 28, $p < 0.05$; comparison of percentage of BL vs vHIP projections, Kolmogorov–Smirnov test, Extinction 5 vs Fear Renewal 5, $D = 0.58$, $p < 0.0001$; Extinction 5 vs Fear renewal 28, $D = 0.69$, $p < 0.0001$; Extinction 5 vs Spontaneous recovery 28, $D = 0.58$, $p < 0.0001$; Spontaneous recovery 28 vs Fear renewal 28, $D = 0.17$, $p = 0.046$). The overall number of anatomic projections did not differ between groups, confirming the behavioral stimulation specificity (Figure 2*E*; Kruskal–Wallis test for BL projections to PL, $H = 1.14$, $p = 0.7961$; for vHIP projections to PL, $H = 4.43$, $p = 0.2268$). Because the overall number of neurons activated in the PL by the retrieval of extinction memory and spontaneous recovery of fear was similar (Fig. 2*F*), different ratios of cells receiving dominant projections from the vHIP or BL suggest that BL-innervated cells are activated instead of vHIP-innervated neurons during fear memory retrieval.

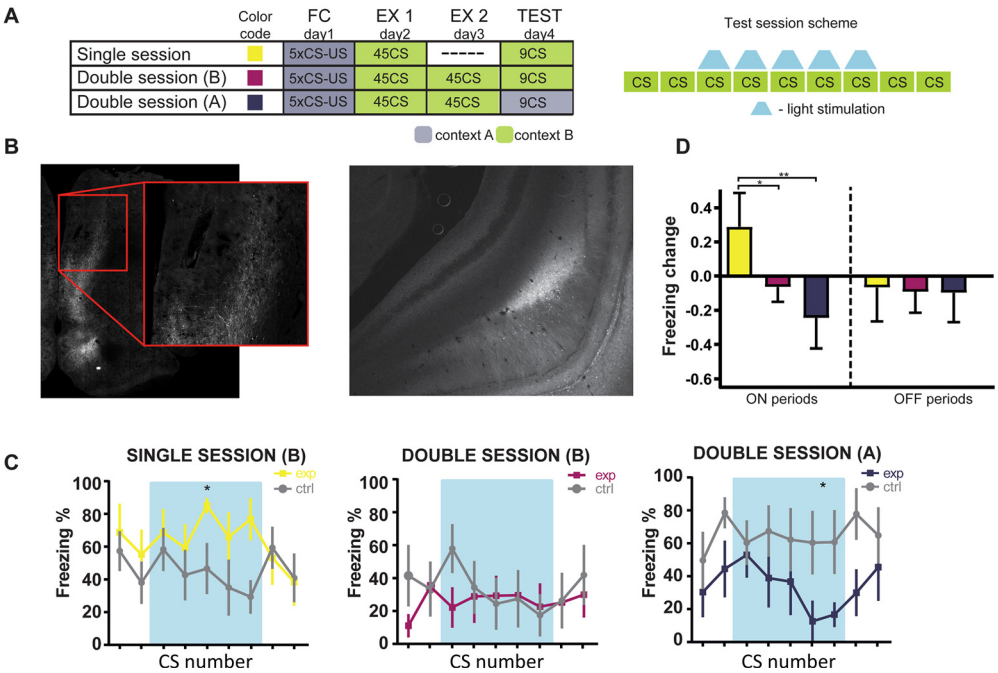

Figure 3. Hippocampal inputs to the PL drive freezing during memory recall. ***A***, Behavioral training scheme and optogenetic design. ***B***, Microphotographs of the optic fiber implantation site in the PL and the CaMKIIα-hChR2 injection site in the vHIP. ***C***, Between-group comparisons during the optogenetic stimulation of the vHIP–PL pathway (blue shadow, ON periods) and without the stimulation (OFF periods). ***D***, Change in freezing in response to the CS expressed as a difference between freezing averaged across CS1–CS5 ON periods or OFF3–OFF4 periods and initial freezing during OFF1–OFF2. Number of animals, Single Session $n = 5/6$; Double Session (B) $n = 6/6$ and Double Session (A) $n = 6/6$; exp/ctrl groups. Error bars indicate mean ± SEM; $*p < 0.05$, $**p < 0.01$. Ctrl, Control; Exp, experimental; FC, fear conditioning; EX, fear extinction.

To test the role of the projections from the vHIP to the PL in retrieval of fear and fear extinction memory we examined the behavioral effects of their optogenetic stimulation. Rats injected with the CaMKIIα-hChR2 virus in the vHIP were implanted with optic fibers in the PL and received light stimulation (Fig. 3). The control group consisted of rats injected with the control virus not containing channelorhodopsin. The rats were subjected to either one or two extinction sessions and tested in extinction context B. Additionally, the rats with two extinction sessions were subsequently tested in conditioning context A. The protocol of stimulation consisted of three blocks of 2 CSs with light off and 5 CSs with light on, which allowed for within-subject comparisons of the activation effects (Fig. 3*A*,*B*). As the effects of the optogenetic stimulation were visible only in the first block of stimuli, we further analyzed data only for this block (including the following CSs: OFF1–OFF2–ON1–ON2–ON3–ON4–ON5–OFF3–OFF4). Activation of the vHIP–PL projections increased the level of fear in the extinction context B when tested shortly after the first extinction session on the fifth day of the experiment, compared with the control group (Fig. 3*C*; two-way ANOVA with repeated measures, group effect, $F_{(1,9)} = 9.35$, $p = 0.0114$). In contrast to stimulation after one extinction session, stimulation of vHIP inputs after two extinction sessions conducted over the course of 2 d did not result in an increase of freezing level in context B (two-way ANOVA with repeated measures, group effect, $F_{(1,10)} = 0.40$, $p = 0.5427$). Subsequent testing in context A revealed slightly decreased freezing in the experimental group (two-way ANOVA with repeated measures, group effect, $F_{(1,10)} = 4.97$, $p = 0.0499$).

Next, to compare changes in freezing to the initial freezing level recorded during the first two OFF periods, we subtracted the averaged freezing to OFF1–OFF2 from the freezing averaged across CS1–CS5 ON or OFF3–OFF4 stimuli (Fig. 3*D*). The stimulation of the vHIP-PL pathway after one session of fear extinction had different effects than stimulation after two sessions of extinction. After one extinction session freezing was increased in the ON periods, and after two extinction sessions there was no change in freezing in context B and a decrease in freezing in context A in the ON periods. No change in the OFF periods was observed (two-way ANOVA with repeated measures, group effect, $F_{(2,14)} = 8.74$, $p = 0.0034$, followed by Newman–Keuls multiple comparisons test, one session vs two sessions, context B in ON periods, $p < 0.05$; one session vs two sessions, context A in ON periods, $p < 0.01$).

To further test the role of the vHIP–PL projections in the retrieval of fear and fear extinction memory we examined the behavioral effects of the optogenetic stimulation using a different experimental design. Rats were injected with the CaMKIIα-hChR2 virus in the vHIP and implanted with optic fibers in the PL as before, but the protocol of light stimulation consisted of 5 CSs with light off and 5 CSs with light on (Fig. 4*A*), subsequently. The control group consisted of rats injected with the control virus not containing channelorhodopsin. First, we tested the level of freezing in rats that were not subjected to fear extinction. There was no significant change in the freezing level during the optogenetic stimulation neither in context B (Fig. 4*B*) nor in context A (data not shown). Because the level of freezing was very high, which makes it difficult to observe an increase in freezing, we performed an additional test in context B. We did not stimulate the vHIP–PL pathway during this session to check for the effects of the previous stimulation on the initial freezing level and extinction rate. The freezing response in both the experimental and control groups gradually decreased, which shows that fear extinction had already begun (Fig. 4*B*). Importantly, however, in line with our previous results, at the beginning of the session we observed higher freezing levels in rats in which we

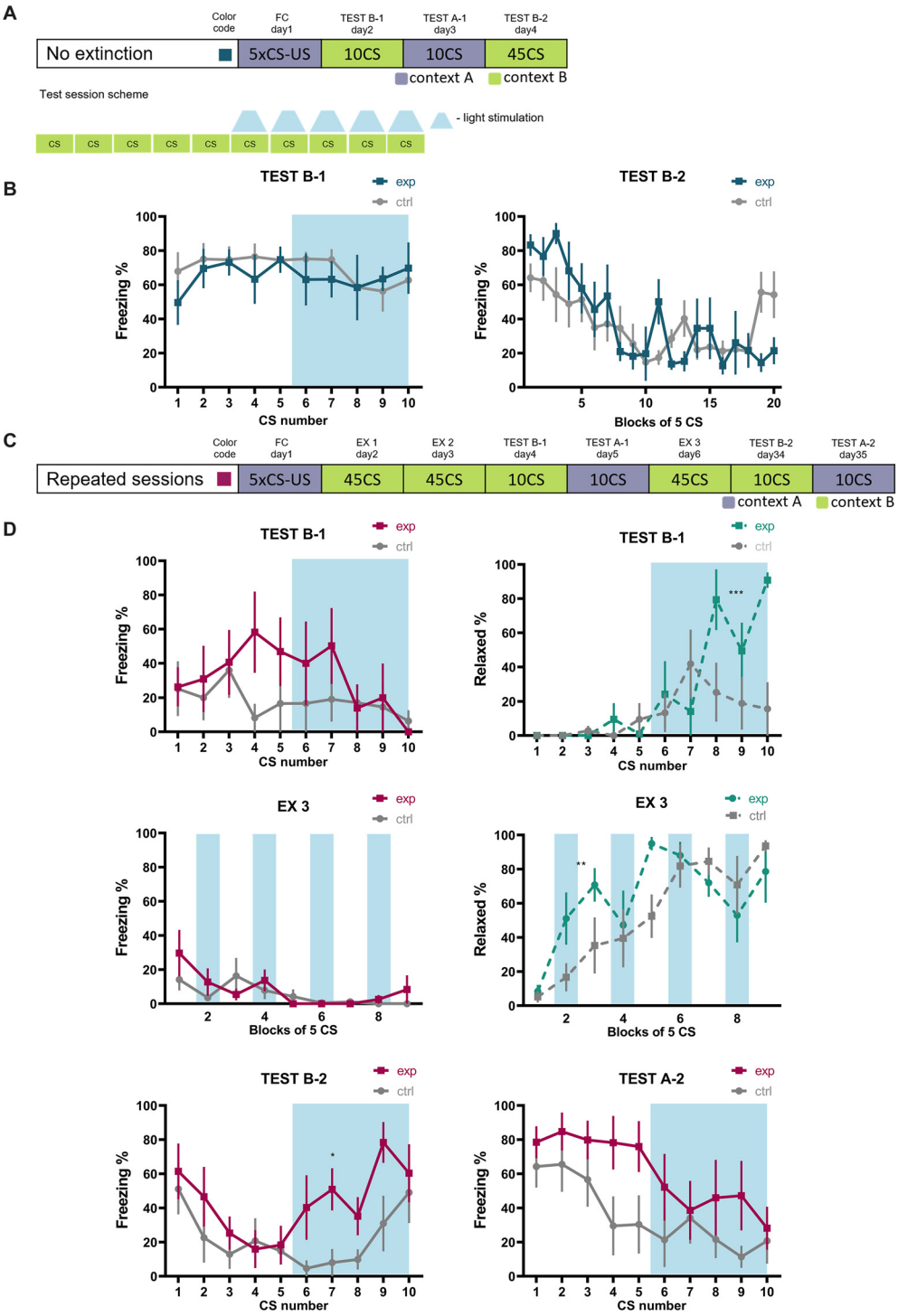

Figure 4. Hippocampal inputs to the PL reduce fear after extinction but this effect is transient. ***A***, Behavioral training scheme and optogenetic stimulation design for the group of rats not subjected to fear extinction. ***B***, The effects of the optogenetic stimulation of the vHIP–PL pathway without prior extinction (exp: $n = 5$, ctrl: $n = 6$), with the light stimulation during test B-1 and without the light stimulation during the subsequent test B-2. The time of light stimulation is marked in blue shadow. ***C***, Behavioral training scheme and optogenetic stimulation design for the group of rats subjected to fear extinction. ***D***, The effects of the optogenetic stimulation of the vHIP–PL pathway with prior extinction (exp: $n = 5$, ctrl: $n = 8$). The graphs show freezing levels (purple) and relaxed posture (green) during the test in context B (test B-1) and the subsequent extinction session (EXT 3), and the freezing levels measured 28 d after the last extinction session in contexts B (B-2) and A (A-2). The time of light stimulation is marked in blue shadow. The data on Ext 3 are shown in blocks of five CSs. Error bars indicate mean ± SEM; $^{*}p < 0.05$, $^{**}p < 0.01$. $^{***}p < 0.001$. Ctrl, Control; Exp, experimental; FC, Fear conditioning; EX, fear extinction.

previously stimulated the vHIP–PL pathway (two-way ANOVA with repeated measures, group × CS effect, $F_{(19,209)} = 1.91$, $p = 0.015$). The extinction rate was similar in both groups, the rats previously stimulated had even slightly lower levels of freezing at the end of the extinction session, which shows that the vHIP–PL stimulation on the previous day did not impede fear extinction.

In another group of rats, we tested the effects of stimulation of the vHIP–PL pathway after two sessions of extinction (Fig. 4*C*,*D*). During the test in extinction context B, we observed a

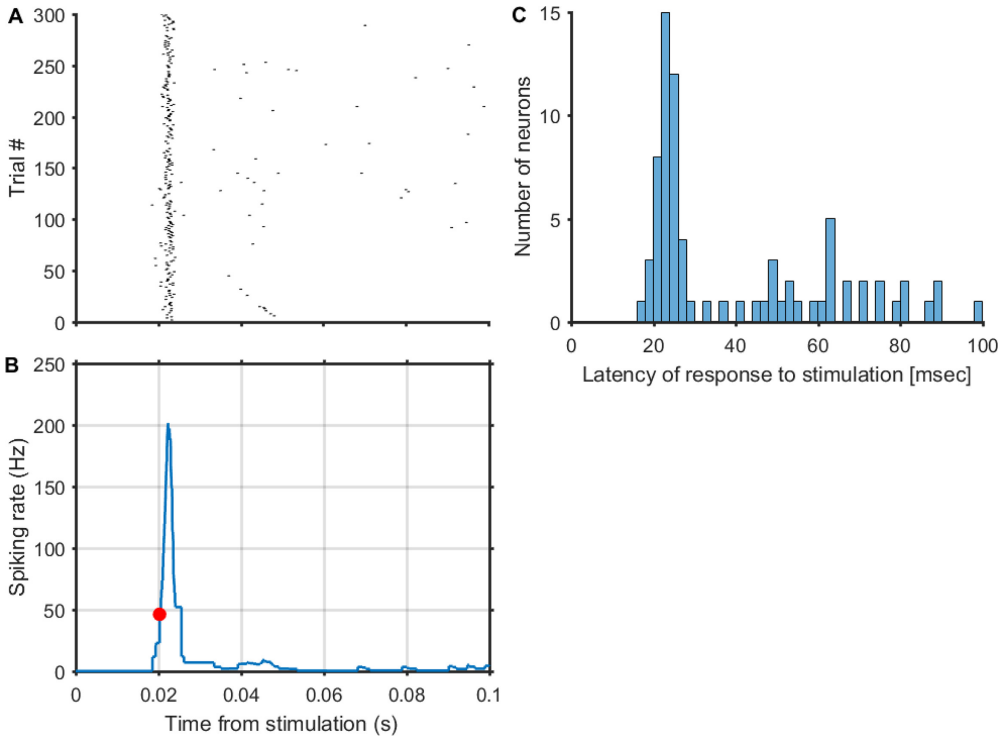

Figure 5. Responses of the mPFC neurons to the electrical vHIP stimulation in urethane-anaesthetized rat. ***A***, Raster plot showing responses of an individual mPFC neuron (# - trial number). ***B***, Instantaneous firing rate calculated for this neuron. The red point represents the latency of the response. ***C***, Distribution of response latencies for all neurons whose activity was regulated by the stimulation ($n = 76$, 30% from 255 recorded in total).

very low level of freezing, thus we focused on another behavioral measure, the relaxed posture, which has been previously used to assess the progress of fear extinction (Tang et al., 2001; see above, Materials and Methods for definition; Fig. 4). We observed that when the vHIP–PL pathway was stimulated, the rats expressed more of the relaxed posture behavior than the animals from the control group (two-way ANOVA with repeated measures, group × CS effect, $F_{(9,81)} = 4.604$, $p < 0.0001$). There was no significant difference between the groups when the vHIP–PL pathway was stimulated in context A (data not shown). Then we tested the effects of the vHIP–PL pathway stimulation in blocks of five CSs with light on during the extinction session, again focusing on the relaxed posture behavior because the level of freezing was very low (Fig. 4*D*). As in the previous tests, stimulation of the vHIP–PL pathway led to increased relaxed posture behavior, which persisted even in the OFF periods (two-way ANOVA with repeated measures, group × CS effect, $F_{(44,396)} = 1.65$, $p = 0.0074$). To test whether the effects of the vHIP–PL stimulation after extinction lasts for a longer time we tested the same animals after 28 d (Fig. 4*D*). Testing in context B revealed increased freezing levels when the vHIP–PL pathway was stimulated (two-way ANOVA with repeated measures, group effect, $F_{(1,9)} = 5.97$, $p = 0.0371$). There were no differences between the groups when the vHIP–PL pathway was stimulated in context A. These results show that the fear-reducing effects of the vHIP–PL pathway stimulation did not persist over time.

Because the data suggested slowly developing modulatory effects of the vHIP–PL pathway, we recorded responses of the cortical neurons to the electrical vHIP stimulation to verify this hypothesis (Fig. 5). The results confirmed the relatively high response latencies of neurons whose activity was regulated by the stimulation (Fig. 5*C*).

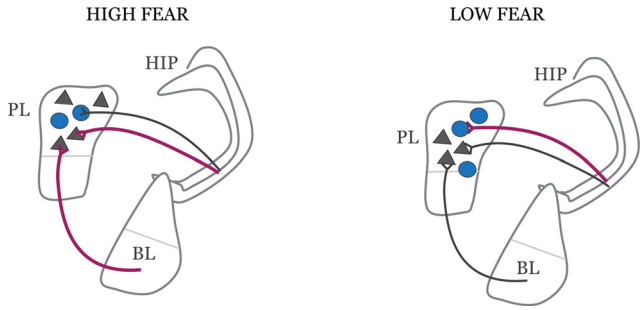

Figure 6. The proposed role of the basolateral and hippocampal projections to the PL. When fear responses are not well extinguished or in case of spontaneous recovery, the projections from both the BL and vHIP are actively increasing freezing response. In contrast, when fear response is well extinguished, the dominant input comes from the vHIP, and it decreases fear response (probably via interneurons). Active projections are marked in purple, pyramidal cells are marked as gray triangles, interneurons as blue circles.

Discussion

In this study, we found two distinct subpopulations of neurons within the PL that are activated by either the retrieval of extinction memory or spontaneous recovery and context-dependent renewal of conditioned fear. They can be distinguished by the projections they receive from the vHIP and BL. The neuronal circuit in the PL whose activity is correlated with retrieval of extinction memory receives input mainly from the vHIP (low fear circuit), whereas the neurons whose activity is correlated with elevated freezing during spontaneous recovery and fear renewal are preferentially innervated by the BL (high fear circuit). The functional mapping findings are supported by the results of the optogenetic stimulation of the vHIP inputs to the PL. They show

that with the sufficient amount of fear extinction, stimulation of the vHIP–PL pathway can decrease the conditioned fear response. Further, they show that fear suppression develops gradually as extinction training progresses, suggesting increasing participation of the inhibitory vHIP inputs when fear extinction memory is being consolidated. In the absence of this fear suppressing input, signals from the BL can play a dominant role, resulting in high levels of fear.

We observed that the high fear neuronal circuit in the PL receives dominant projections from the BL. This agrees well with previous reports, which showed that the BL–PL pathway plays an important role in conditioned freezing (Herry et al., 2008; Sotres-Bayon et al., 2012; Senn et al., 2014; Kim et al., 2016) and the model proposed by Pendyam et al. (2013), in which the activity in the BL–PL pathway is associated with retrieval of conditioned fear response. Our results are also in accordance with those of Klavir et al. (2017), who showed the importance of the BL inputs to the PL in forming and maintaining cued fear associations. Importantly, we observed activation of this pathway regardless of the age of fear memory and testing context, that is, both in fear renewal groups tested 1 and 28 d after fear conditioning in the conditioning context and in the spontaneous recovery group tested 28 d after conditioning in the extinction context.

We found that, in contrast to the BL–PL pathway, the vHIP–PL projections were activated when rats showed low levels of fear. This result is at odds with earlier reports showing involvement of the vHIP–PL pathway in conditioned fear renewal (Orsini et al., 2011; Jin and Maren, 2015; Wang et al., 2016; Kim and Cho, 2017) and in anxiety (Adhikari, 2010; Ciocchi et al., 2015; Padilla-Coreano et al., 2016) rather than in suppression of fear. However, Sotres-Bayon et al. (2012) observed that the vHIP inactivation decreased activity of interneurons in the PL and increased PL responses to the conditioned tone in extinguished but not in conditioned rats, suggesting that the vHIP inputs to the PL can gate fear expression after extinction. Moreover, a published report shows that both in mice and humans, the vHIP–PL pathway is involved in conditioned inhibition of threat by safety signals (Meyer et al., 2019). Also, it has been shown that projections from the superficial layer of vHIP, which terminate on inhibitory interneurons in the PL, promote exploration, whereas projections from the deep layers of vHIP terminating on the pyramidal cells and fast-spiking interneurons promote avoidance (Sánchez-Bellot and MacAskill, 2019). It seems plausible that the prolonged extinction training we used strengthened the projections promoting exploration, whereas in animals not subjected to fear extinction or subjected to the short extinction protocol, we observed the effects of stimulation of the projections promoting defensive responses. This would suggest that the vHIP to PL projections gate fear renewal, spontaneous recovery, and extinction memory via different neuronal subpopulations (compare Fig. 6). Together, the discrepancies in the literature on the role of the vHIP–PL pathway in fear memory and extinction memory retrieval may stem from the amount of extinction training, a factor that has not been systematically tested before. Here, we found that only well-consolidated extinction memory allows for decreasing of conditioned fear through the stimulation of the vHIP–PL pathway and that over time the same stimulation boosts spontaneous recovery of fear. On the other hand, the lack of extinction or insufficient extinction leads to increased freezing when the vHIP–PL pathway is stimulated. Additionally, we observed delayed behavioral change to the laser simulation. As the vHIP to PL pathway is not the only pathway that contributes to the modulation of fear expression (e.g., the other pathways are BL to PL and PL to infralimbic cortex), this effect can result from synergy between activation of different pathways, which are gradually recruited.

We hypothesize that by activating the vHIP–PL pathway after prolonged extinction, we accelerated the relaxed posture display by modulating PL activity, which effectively decreased the response to conditioned tone because of consolidated memory of extinction and lower BL activation (Gale, 2004). Furthermore, it has been shown that neurons projecting from the vHIP to both the BL and PL are involved in contextual fear renewal (Jin and Maren, 2015; Kim and Cho, 2017). This is in line with previous reports showing that fear renewal is mediated by vHIP–BL projections (Herry et al., 2008; Lesting et al., 2011; Knapska et al., 2012; Jin and Maren, 2015) and supports the hypothesis concerning anatomically diverse populations of neurons in the vHIP upregulating and downregulating fear responses. The hypothesis is also supported by the results of Sánchez-Bellot and MacAskill (2019), who identified calbindin-positive neurons in the superficial layers of the vHIP projecting onto interneurons in the PL and deep-layer vHIP neurons projecting onto pyramidal neurons and surrounding interneurons.

Our optogenetic results suggest that the inhibitory part of the vHIP–PL pathway is a modulatory connection, which needs more training to be formed and if not behaviorally maintained weakens over time to the point that extinction memory is no longer effectively retrieved, and fear re-emerges. This hypothesis is consistent with the observation that synaptic efficacy in the vHIP–PL pathway is not stable after the extinction training, it is increased when a memory is 1 d old but not 7 d after the initial extinction (Hugues and Garcia, 2007). Previous findings suggest that the vHIP–PL pathway has a relatively high latency of ~20 msec (Ishikawa and Nakamura, 2003) with long hyperpolarization induced by glutamatergic input onto GABAergic interneurons (Thierry et al., 2000), which suggests the slowly developing, modulatory effects of the pathway. Our results confirm long response latencies of the cortical neurons after vHIP stimulation.

Changes in physical or temporal context have been suggested to account for fear renewal and spontaneous recovery (Pavlov, 1927; Bouton, 1993, 2002; Quirk, 2002; Rescorla, 2004; Maren et al., 2013). However, the neural mechanisms underlying these two forms of recovery of extinguished fear are not well understood. The involvement of the specific brain circuits was studied mainly during the initial processing of fear extinction memory and its contextual modulation (Frankland et al., 2004, Frankland and Bontempi 2005, Goshen et al., 2011; Do-Monte et al., 2015). Here, we generated functional maps of the neural circuits involved in the contextual retrieval of recent and remote fear memory after extinction and systematically compared the patterns of activation and connectivity of the PL, vHIP, and BL. The results show that the activation of the BL input to the PL is a common mechanism for both fear renewal and spontaneous recovery of fear. Interestingly, activation of the vHIP projections to the PL boosts spontaneous recovery of fear but does not affect remote fear renewal.

Fear recovery is a major obstacle in effective, long-lasting treatment of pathologic fear (Boschen et al., 2009; Goode and Maren, 2014). Identifying the neural networks involved in regulating fear memory after extinction is essential for the development of more effective therapeutic interventions. Because the dorsal anterior

cingulate cortex, a homolog of the rodent PL is hyperactive, and the anterior hippocampus, a homolog of the rodent vHIP, shows decreased activity in cases of pathologic fear (Milad et al., 2009), targeting the hippocampal–dorsal ACC gating circuit seems to be a promising way to treat fear regulation deficits. Our results show, however, that stimulation of this circuit may decrease fear only when it is already sufficiently extinguishes, for example, by exposure therapy.

References

Adhikari A, Topiwala MA, Gordon JA (2010) Synchronized activity between the ventral hippocampus and the medial prefrontal cortex during anxiety. Neuron 65:257–269.

Barad M, Gean P-W, Lutz B (2006) The role of the amygdala in the extinction of conditioned fear. Biol Psychiatry 60:322–328.

Boschen MJ, Neumann DL, Waters AM (2009) Relapse of successfully treated anxiety and fear: theoretical issues and recommendations for clinical practice. Aust N Z J Psychiatry 43:89–100.

Bouton ME (1993) Context, time, and memory retrieval in the interference paradigms of Pavlovian learning. Psychol Bull 114:80–99.

Bouton ME (2002) Context, ambiguity, and unlearning: sources of relapse after behavioral extinction. Biol Psychiatry 52:976–986.

Bouton ME (2004) Context and behavioral processes in extinction. Learning & Memory 11:485–494.

Bouton ME, Westbrook RF, Corcoran KA, Maren S (2006) Contextual and temporal modulation of extinction: behavioral and biological mechanisms. Biol Psychiatry 60:352–360.

Burgos-Robles A, Vidal-Gonzalez I, Quirk GJ (2009) Sustained conditioned responses in prelimbic prefrontal neurons are correlated with fear expression and extinction failure. J Neurosci 29:8474–8482.

Ciocchi S, Passecker J, Malagon-Vina H, Mikus N, Klausberger T (2015) Selective information routing by ventral hippocampal CA1 projection neurons. Science 348:560–563.

Do-Monte FH, Quiñones-Laracuente K, Quirk GJ (2015) A temporal shift in the circuits mediating retrieval of fear memory. Nature 519:460–463.

Fanselow MS, LeDoux JE (1999) Why we think plasticity underlying pavlovian fear conditioning occurs in the basolateral amygdala. Neuron 23:229–232.

Frankland PW, Bontempi B (2005) The organization of recent and remote memories. Nat Rev Neurosci 6:119–130.

Frankland PW, Bontempi B, Talton LE, Kaczmarek L, Silva AJ (2004) The involvement of the anterior cingulate cortex in remote contextual fear memory. Science 304:881–883.

Gale GD, Anagnostaras SG, Godsil BP, Mitchell S, Nozawa T, Sage JR, Wiltgen B, Fanselow MS (2004) Role of the basolateral amygdala in the storage of fear memories across the adult lifetime of rats. J Neurosci 24:3810–3815.

Giustino TF, Maren S (2015) The role of the medial prefrontal cortex in the conditioning and extinction of fear. Front Behav Neurosci 9:298.

Goode TD, Maren S (2014) Animal models of fear relapse. ILAR J 55:246–258.

Goshen I, Brodsky M, Prakash R, Wallace J, Gradinaru V, Ramakrishnan C, Deisseroth K (2011) Dynamics of retrieval strategies for remote memories. Cell 147:678–689.

Herry C, Ciocchi S, Senn V, Demmou L, Müller C, Lüthi A (2008) Switching on and off fear by distinct neuronal circuits. Nature 454:600–606.

Hoover WB, Vertes RP (2007) Anatomical analysis of afferent projections to the medial prefrontal cortex in the rat. Brain Struct Funct 212:149–179.

Hugues S, Garcia R (2007) Reorganization of learning-associated prefrontal synaptic plasticity between the recall of recent and remote fear extinction memory. Learn Mem 14:520–524.

Ishikawa A, Nakamura S (2003) Convergence and interaction of hippocampal and amygdalar projections within the prefrontal cortex in the rat. J Neurosci 23:9987–9995.

Ji J, Maren S (2007) Hippocampal involvement in contextual modulation of fear extinction. Hippocampus 17:749–758.

Jin J, Maren S (2015) Prefrontal-hippocampal interactions in memory and emotion. Front Syst Neurosci 9:170.

Kim J, Pignatelli M, Xu S, Itohara S, Tonegawa S (2016) Antagonistic negative and positive neurons of the basolateral amygdala. Nat Neurosci 19:1636–1646.

Kim WB, Cho JH (2017) Synaptic targeting of double-projecting ventral CA1 hippocampal neurons to the medial prefrontal cortex and basal amygdala. J Neurosci 37:4868–4882.

Klavir O, Prigge M, Sarel A, Paz R, Yizhar O (2017) Manipulating fear associations via optogenetic modulation of amygdala inputs to prefrontal cortex. Nat Neurosci 20:836–844.

Knapska E, Maren S (2009) Reciprocal patterns of c-*fos* expression in the medial prefrontal cortex and amygdala after extinction and renewal of conditioned fear. Learn Mem 16:486–493.

Knapska E, Macias M, Mikosz M, Nowak A, Owczarek D, Wawrzyniak M, Pieprzyk M, Cymerman IA, Werka T, Sheng M, Maren S, Jaworski J, Kaczmarek L (2012) Functional anatomy of neural circuits regulating fear and extinction. Proc Natl Acad Sci U S A 109:17093–17098.

Konorski J (1948) Conditioned reflexes and neuronal organization. London: Cambridge UP.

Lesting J, Narayanan RT, Kluge C, Sangha S, Seidenbecher T, Pape H-C (2011) Patterns of coupled theta activity in amygdala-hippocampal-prefrontal cortical circuits during fear extinction. PLoS One 6:e21714.

Maren S (2011) Seeking a spotless mind: extinction, deconsolidation, and erasure of fear memory. Neuron 70:830–845.

Maren S, Phan KL, Liberzon I (2013) The contextual brain: implications for fear conditioning, extinction and psychopathology. Nat Rev Neurosci 14:417–428.

Meyer HC, Odriozola P, Cohodes EM, Mandell JD, Li A, Yang R, Lee FS (2019) Ventral hippocampus interacts with prelimbic cortex during inhibition of threat response via learned safety in both mice and humans. Proc Natl Acad Sci U S A 116:26970–26979.

Milad MR, Pitman RK, Ellis CB, Gold AL, Shin LM, Lasko NB, Zeidan MA, Handwerger K, Orr SP, Rauch SL (2009) Neurobiological basis of failure to recall extinction memory in posttraumatic stress disorder. Biol Psychiatry 66:1075–1082.

Montijn JS, Seignette K, Howlett MH, Cazemier JL, Kamermans M, Levelt CN, Heimel JA (2020) A parameter-free statistical test that improves the detection of neuronal responsiveness. bioRxiv 311118. doi: https://doi.org/10.1101/2020.09.24.311118.

Ohman A, Eriksson A, Olofsson C (1975) One-trial learning and superior resistance to extinction of autonomic responses conditioned to potentially phobic stimuli. J Comp Physiol Psychol 88:619–627.

Orsini CA, Kim JH, Knapska E, Maren S (2011) Hippocampal and prefrontal projections to the basal amygdala mediate contextual regulation of fear after extinction. J Neurosci 31:17269–17277.

Padilla-Coreano N, Bolkan SS, Pierce GM, Blackman DR, Hardin WD, Garcia-Garcia AL, Spellman TJ, Gordon JA (2016) Direct ventral hippocampal-prefrontal input is required for anxiety-related neural activity and behavior. Neuron 89:857–866.

Parfitt GM, Nguyen R, Bang JY, Aqrabawi AJ, Tran MM, Seo DK, Richards BA, Kim JC (2017) Bidirectional control of anxiety-related behaviors in mice: role of inputs arising from the ventral hippocampus to the lateral septum and medial prefrontal cortex. Neuropsychopharmacology 42:1715–1728.

Paxinos G, Watson C (2006) The rat brain in stereotaxic coordinates: hard cover edition. Elsevier.

Pavlov IP (1927) Conditioned reflexes. London: Oxford UP.

Pendyam S, Bravo-Rivera C, Burgos-Robles A, Sotres-Bayon F, Quirk GJ, Nair SS (2013) Fear signaling in the prelimbic-amygdala circuit: a computational modeling and recording study. J Neurophysiol 110:844–861.

Quirk GJ (2002) Memory for extinction of conditioned fear is long-lasting and persists following spontaneous recovery. Learn Mem 9:402–407.

Rescorla RA (2004) Spontaneous recovery. Learn Mem 11:501–509.

Sánchez-Bellot C, MacAskill Push AF (2019) Push-pull regulation of exploratory behavior by two opposing hippocampal to prefrontal cortex pathways. bioRxiv 880831. doi: 10.1101/2019.12.18.880831.

Senn V, Wolff SBE, Herry C, Grenier F, Ehrlich I, Gründemann J, Fadok JP, Müller C, Letzkus JJ, Lüthi A (2014) Long-range connectivity defines behavioral specificity of amygdala neurons. Neuron 81:428–437.

Sierra-Mercado D, Padilla-Coreano N, Quirk GJ (2011) Dissociable roles of prelimbic and infralimbic cortices, ventral hippocampus, and basolateral amygdala in the expression and extinction of conditioned fear. Neuropsychopharmacology 36:529–538.

Sotres-Bayon F, Sierra-Mercado D, Pardilla-Delgado E, Quirk GJ (2012) Gating of fear in prelimbic cortex by hippocampal and amygdala inputs. Neuron 76:804–812.

Tang J, Wotjak CT, Wagner S, Williams G, Schachner M, Dityatev A (2001) Potentiated amygdaloid auditory-evoked potentials and freezing behavior after fear conditioning in mice. Brain Res 919:232–241.

Thierry A-M, Gioanni Y, Dégénétais E, Glowinski J (2000) Hippocampo-prefrontal cortex pathway: anatomical and electrophysiological characteristics. Hippocampus 10:411–419.

Vasquez JH, Leong KC, Gagliardi CM, Harland B, Apicella AJ, Muzzio IA (2019) Pathway specific activation of ventral hippocampal cells projecting to the prelimbic cortex diminishes fear renewal. Neurobiol Learn Mem 161:63–71.

Wang Q, Jin J, Maren S (2016) Renewal of extinguished fear activates ventral hippocampal neurons projecting to the prelimbic and infralimbic cortices in rats. Neurobiol Learn Mem 134 Pt A:38–43.